Hindawi
International Journal of Antennas and Propagation
Volume 2021, Article ID 8874385, 11 pages
https://doi.org/10.1155/2021/8874385

Research Article

Optimization of Modified Yagi-Uda Nanoantenna Arrays Using Adaptive Fuzzy GAPSO

Pitther N. Santos, Victor Dmitriev, and Karlo Q. da Costa

Department of Electrical Engineering, Federal University of Para, Belém-PA, Brazil

Correspondence should be addressed to Pitther N. Santos; pitther.negrao@yahoo.com.br

Received 18 September 2020; Revised 23 December 2020; Accepted 21 January 2021; Published 17 February 2021

Academic Editor: Diego Caratelli

Copyright © 2021 Pitther N. Santos et al. This is an open access article distributed under the Creative Commons Attribution License, which permits unrestricted use, distribution, and reproduction in any medium, provided the original work is properly cited.

This paper presents an optimization of the radiation and absorption characteristics of modified Yagi-Uda (YU) nanoantenna arrays. Four geometries of antennas are considered: conventional YU fed by voltage source and transmission line, and YU with a loop element fed by voltage source and transmission line. The numerical electromagnetic simulations of these nanoantennas were made by the method of moments (MoM). The optimization method used is the adaptive fuzzy GAPSO, which consists of hybridization between genetic algorithm (GA) and particle swarm optimization (PSO), with a fuzzy system employed to adapt the inertial weight ω and the acceleration coefficients C_1 and C_2 of PSO. The optimized results show that the modified YU nanoantennas present better characteristics of gain, directivity, and radiation efficiency than the conventional YU antenna.

1. Introduction

Optical nanoantennas have received great interest in recent years in the scientific community due to its ability to increase and confine optical fields beyond the diffraction limit of light. With this characteristic, it is possible application in the areas of nanophotonics, biology, chemistry, computer science, optical microscopy, photovoltaic, and others [1–3].

Array of optical antennas, for example, Yagi-Uda (YU) nanoantennas, possess better unidirectional radiation characteristics than single element antennas [4]. Also, these antennas can provide higher coupling between optical fields and nanoplasmonic waveguides [5, 6]. In [7], Mironov et al. fabricated an array of 80 YU nanoantennas on the coating of an optical fiber. This antenna was fed by a Gaussian beam and its radiation was optimized at $\lambda = 1060$ nm, where the authors obtained an increase in directivity around 5 dB. Already in [8], through 3D numerical calculations, the interaction of a single emitter with a YU array is presented. It was proven that the electromagnetic fields from the emitter are improved due the array. Also, a tunable YU nanoantenna with semiconductors material loaded in the gap of the dipole element in the array is shown in [9]. In [10], Da Costa et al. used YU nanoantennas to improve the transmission efficiency of a wireless optical nanolink. In all these works, a little attention has been given to the optimization process of the nanoantennas, i.e., no special optimization technique was used in the antenna design.

This paper proposes the optimization of radiation and absorption of four models of YU nanoantennas. The first model is the classical geometry composed by five cylindrical elements made of gold: a reflector, a dipole, and three directors, where the dipole is fed by an equivalent voltage source. The second model has the same geometry as the first, but the dipole is connected to an optical transmission line (OTL). The third model is a conventional YU combined with a rectangular loop placed above the feeding dipole. The fourth model has the same geometry of the third model, but with an OTL connected to the dipole. These nanoantennas were analyzed numerically by the Method of Moments (MoM) [11], where a MoM code was developed to simulate and optimize these antennas. There are some works about optimization of antennas array available in literature, where different optimization techniques have been used [12–16]. However, we prefer to use in present paper the fuzzy adaptive GAPSO method due their better efficiency [17].

This optimization technique is a hybrid method between genetic algorithm (GA) and particle swarm optimization (PSO), with a fuzzy system used to adapt some parameters of PSO.

The geometries of the proposed antennas were optimized to obtain optimal radiation efficiency and gain and directivity in the frequency range of 100–400 THz. The optimized results are presented and discussed. Some results are compared with simulations made by software based on finite element method [18] in order to compare and validate our results. The remainder of this work is organized as follows. Section 2 presents the geometries of the antennas and the theoretical MoM model considered, Section 3 explains the optimization technique used in this work, and Section 4 presents the numerical results and Section 5 the conclusions.

2. Theoretical Development

2.1. Geometries of the YU Nanoantennas. Figure 1(a) illustrates schematically the considered conventional YU nanoantenna, consisting of a nanodipole, three directors above of nanodipole, and one reflector below it. The entire structure of the model is located in free space. In this figure, a voltage source V_s, applied in the gap d, located in the center of the nanodipole is used to fed the nanoantenna. Figure 1(b) has the same geometry as the previous case, but an optical transmission line (OTL) is connected through the dipole. The only difference between a standard transmission line and an OTL is the physical properties of the conductors. The conductivity of metals is not infinite in optical frequencies, that is, the metal presents a complex permittivity variable with frequency. In other words, the metals not behave like perfect conductors, but rather as plasmonic material described by the Lorentz–Drude model for the complex permittivity. This OTL is perpendicular to the plane of the array and placed along the axis z. The third antenna shown in Figure 1(c) is a YU nanoantenna combined with a rectangular loop, which is fed by a voltage source V_s. The loop element is centered symmetrically with the dipole, in respect to the xy plane but is located above it by a distance d_w in direction of axis z, not shown in this figure. Figure 1(d) is the same YU nanoantenna as the previous case but connected to an OTL.

The geometric parameters of the nanoantennas are as follows: for the dipole, arm length (h), radius (a_h), and feed gap (d); for the reflector, length (h_r), radius (a_r), and distance to dipole (d_h); for the directors, length (h_n) radius (a_n), and distance to the previous director or dipole; in the case of the first director, d_n for $n = 1$, 2, and 3; for the OTL, length (L) and radius (a_l); and for the loop, length (h_e), width (w_e), height (d_w), and radius (a_e). The antenna arrays are in the xy plane with the dipole aligned along the y axis and the axis of the array aligned in the x direction as illustrated in Figure 1.

2.2. Method of Moments Model. The method of moments (MoM) is a technique used to solve the integral equation 1 D of the electric field, with linear approximation of the current longitudinal, rectangular pulse for test functions, and sinusoidal base functions [11]. The radiation problem of the nanoantennas in Figure 1 consists of an incident electric field $\overline{E}_i$ radiated from a voltage source in the center of the nanodipole or at the beginning of the OTL. This voltage generates an induced electric current I_{in} the conductors who in turn will radiate a field $\overline{E}_s$. The integral equation of electric field is obtained substituting the scattered field and the incident filed in the boundary conditions on the metal's surface [11]:

$$\left(\overline{E}_s + \overline{E}_i\right) \cdot \overline{a}_l = Z_s I, \tag{1}$$

where $\overline{a}_t$ is a unit vector tangent to the surface of the conductors, I is the current in a particular point on the nanoantenna's surface, and Z_s is the surface impedance of the conductors. The metallic nanoantenna is made of gold, where the model of its complex permittivity is the LorentzDrude model [19], given by

$$\varepsilon_{r1} = \varepsilon_\infty - \frac{\omega_{p1}^2}{\omega^2 - j\Gamma_D\omega} + \frac{\omega_{p2}^2}{\omega_0^2 - \omega^2 + j\gamma_L\omega}, \tag{2}$$

where the constants are $\omega_0 = 2\pi c/\lambda_0$, $\lambda_0 = 450\,\text{nm}$, and $c = 3 \times 10^8$ m/s, $\varepsilon_\infty = 8$, $\omega_{p1} = 13.8 \times 10^{15}\,\text{s}^{-1}$, $\omega_{p2} = 45 \times 10^{14}\,\text{s}^{-1}$, $\Gamma_D = 1.075 \times 10^{14}\,\text{s}^{-1}$, and $\gamma_D = 9 \times 10^{14}\,\text{s}^{-1}$. We can calculate the surface impedance by [20]

$$\begin{aligned} Z_s &= \frac{T, J_0\,(\text{Ta})}{2\pi a j\omega\varepsilon_1 J_1\,(\text{Ta})}, \\ T &= k_0\sqrt{\varepsilon_{r1}}, \\ k_0 &= \omega\sqrt{\mu_0\varepsilon_0}, \\ \varepsilon_1 &= \varepsilon_0\varepsilon_{r1}, \end{aligned} \tag{3}$$

where J_0 and J_1 are the Bessel functions of first type and zero order, respectively, j is the imaginary unit, ω the frequency of operation, and $T = k_0\sqrt{\varepsilon - (\beta/k_0)^2}$, β being the phase constant in the cylindrical waveguide, $k_0 = \omega\sqrt{\mu_0\varepsilon_0}$ the propagations constant in the air, μ_0 the magnetic permeability of air, and $\varepsilon_0$the electrical permittivity of air.

To transform the integral equation (1) in a linear system, we apply the conventional linear MoM with base functions sine and test functions rectangular pulse [11], where the following linear system is obtained:

$$V_m = Z_s I_m \Delta_m + \sum_{n=1}^{N} Z_{mn} I_n, \quad m = 1, 2, \ldots, N-1, \tag{4}$$

where V_m is the voltage in one generic segment m, the elements of Z_{mn} represent the mutual impedance between different points m and n on the antenna's surface, Δ_m is the length of each segment, and N is the total number of segments. The solution of the system (4) produces the current distribution I_m, and by this current, it is possible to calculate all the radiation and absorptions characteristics. All these parameters have been defined in [11]. The input impedance is calculated by

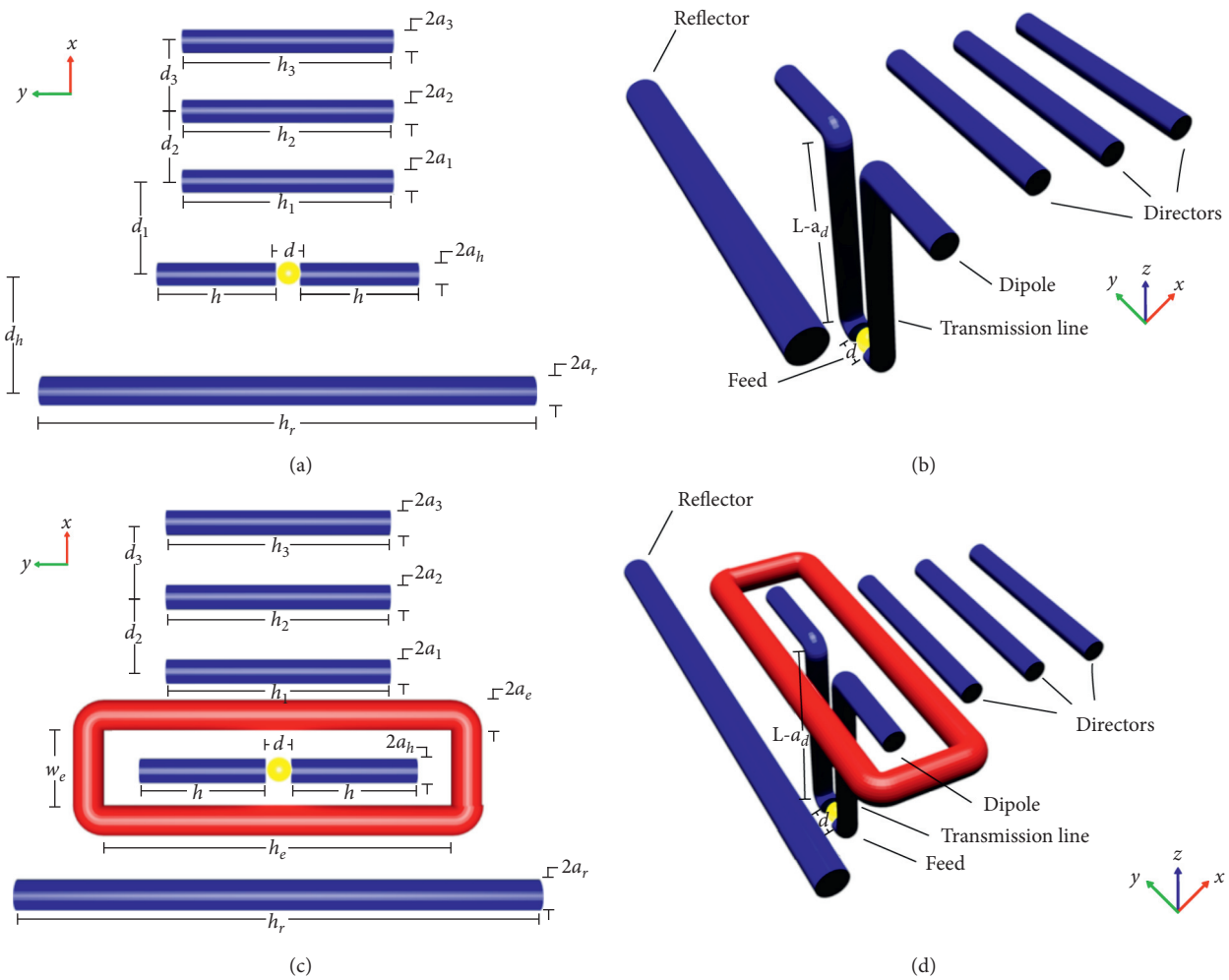

Figure 1: Geometries of the four YU nanoantennas models in study. (a) Conventional YU, (b) YU with OTL, (c) YU with loop, and (d) YU with loop and OTL.

$$Z_{in} = \frac{V_s}{I_f}, I_f = \frac{1}{\sinh \lambda d}\left[I_s \sinh\frac{\gamma d}{2} + I_{s+1}\sinh\frac{\gamma d}{2}\right], \quad (5)$$

where the localization of the voltage source is $m = s$. For $V_s = 1\ V$, the input impedance is $Z_{in} = 1/I_f = (R_r + R_L) + jX_{in} = R_{in} + jX_{in}$, where R_r, R_L, R_{in}, and X_{in} are the radiation resistance, loss resistance, input resistance, and input reactance, respectively. The total input power is calculated by $P_{in} = 0.5\,\mathrm{Re}\ (V_s I_f *) = 0.5\,(R_L + R_r)|I_f|^2 = 0.5\,R_{in}|I_f|^2 = P_r + P_L$, P_r is the radiated power and P_L the loss power dissipated at the antenna's surface which is calculated by [11]

$$P_L = 0.5\mathrm{Re}(Z_s)\sum_{n=1}^{N-1}|I_n|^2\Delta_n. \quad (6)$$

The radiated power can be obtained by $P_r = P_{in} - P_L$ and the resistances by $R_r = 2P_r/|I_f|^2$ and $R_L = 2P_L/|I_f|^2$. The radiation efficiency is defined by $e_r = P_r/P_{in} = P_r/(P_r + P_L) = R_r/(R_r + R_L) = R_r/R_{in}$.

3. Hybrid Method Adaptive Fuzzy GAPSO

3.1. Genetic Algorithm. The genetic algorithm (GA) is a metaheuristic inspired in the Darwinian natural selection, where the candidate solutions are represented by individuals, whose parameter vectors are coded in chromosomes and the parameters in each vector are coded in genes. The GA executes iteratively, the procedures of selection, crossover, and mutation in the population to generate individuals with optimized parameters. The selection process consists in selecting, among the population, the individuals who present the best evaluation, according to the objective function, while the remaining ones are discarded. The selection can be done by ranking [21], roulette [22], or tournament [23], and the selection criteria can be a threshold cost value or a determined percentage of population.

The following procedure of crossover consist in the generation of new individuals from the gene recombination among the present individuals called parents to obtain improved solutions by combining the favorable characteristics of the existing solutions. The main crossover methods

applied are as follows: simple crossover [24], arithmetic crossover [25], and uniform crossover [26].

The final procedure mutation changes, with an arbitrary probability, some parameters of the individuals, to generate and preserve diversity in the population and improve the exploration of the search space. The random mutation is the main employed mutation method and consists in randomly choosing individuals from the population and, from the chosen individuals, the genes that will be modified to random values [27].

3.2. Fuzzy Inference System (FIS). FIS are systems that apply fuzzy logic to make inferences from linguistic variables from a fuzzy associative matrix to output the system's response to the given inputs. Such systems are used to deal with parameters that present considerable uncertainty margin and/or have a complex mathematical representation [17]. The FIS are formed by: input variables, pertinence functions, fuzzy associative matrix, and output variables. The input variables are quantities that the FIS receive to generate inferences. The pertinence functions define a relation between a given input/output variable and its linguistic variables and determine how much the input variable is pertinent to each fuzzy set defined for these variables [28]. The fuzzy associative matrix defines the relations among the input and output variables, based on its linguistic variables. From the pertinence values of the input variables, the associative matrix infers the pertinence values of the output variables. The inference method employed in the FIS depends on its classification; the two most used classes of FIS are the Mamdani [28] and Tagaki-Sugeno [29] systems. The output variables receive the pertinence values inferred by the system and, by means of its pertinence functions, determine the real value that correspond to the received pertinence values and return them to the FIS output. From these real values, it is possible to control and adaptively adjust external systems connected to the FIS [28]. In the case of the adaptive fuzzy GAPSO, the FIS is a Mamdani system and is responsible to adjust the acceleration coefficients C_1 and C_2 which are the output variables of the FIS having as input variables: the percentage of complete iterations; and the normalized Euclidian distance defines as the ratio between the mean of the distances among the individual with best evaluation and the remaining individuals and the distance between the most distant individual and the best evaluated individual.

3.3. Particle Swarm Optimization (PSO). The PSO is metaheuristic inspired in the behavior of birds swarms searching for food [30]. The candidate solutions are represented by particles, in which its parameter vectors are coded in the position that each particle occupies in the search space. The particles $i = 1, \ldots, n$ are described by the current position $\overrightarrow{x_i}$ in the search space, the velocity $\overrightarrow{v_i}$, and the best individual position $\overrightarrow{g_i}$ [31]. PSO initially, determines the best individual positions $\overrightarrow{g_i}$, by evaluating the solution contained in each particle and the best global position $\overrightarrow{g_b}$ as the $\overrightarrow{g_i}$ with best evaluation. Then, the PSO updates the velocity $\overrightarrow{v_i}$ of each by [31]:

$$\overrightarrow{v_i} = W^* \overrightarrow{v_i} + \text{rand}^* C_1{}^* \overrightarrow{g_i} + \text{rand}^* C_2{}^* \overrightarrow{g_b}, \tag{7}$$

where W is the inertia coefficient of the particle and quantifies the resistance to changes in velocity presented by the particle; C_1 is the coefficient of individual acceleration, and quantifies the tendency of the particle to move towards its best individual solution; C_2 is the coefficient of social acceleration, and quantifies the tendency of the particle to direct to the best global solution; and rand is a random variable with uniform distribution in the range [0, 1] [30]. With the updated velocity, the final step of particle dislocation is done with [30, 31]

$$\overrightarrow{x_i} = \overrightarrow{x_i} + \overrightarrow{v_i}. \tag{8}$$

3.4. Adaptive Fuzzy GAPSO Method. To perform the optimization, the hybrid method adaptive fuzzy GAPSO was applied [17]. The adaptive fuzzy GAPSO is composed by three different methods that operate together to find an optimal solution for optimization problems. The methods are genetic algorithm (GA), fuzzy inference system (FIS), and particle swarm optimization (PSO).

Initially, the adaptive fuzzy GAPSO generates a population of N individuals, where each individual is represented by a vector of m values; the individuals represent the candidate solutions, and the vectors represent the parameters of each solution. Then, it is defined as the maximum number of iterations n, which will be the stopping criteria of the adaptive fuzzy GAPSO, the objective function (function that evaluates the individual's pertinence), the search space, and the optimization restrictions. After the initial procedures, the adaptive fuzzy GAPSO executes iteratively and in following sequence: the GA, the FIS, and the PSO, generating a new and improved population in each iteration, as is described in the flowchart in Figure 2 and in the following pseudocode.

This pseudocode explains the AGPSO used in this work, where an intermediary solution is obtained in each iteration. The stop condition verifies whether the total number of iterations has been achieved or if the best solution found by AGPSO remains constant in different iterations. If one of these conditions is met, the AGPSO stops and returns the best solution and the cost/relevance value. The population size and other general parameters used in the AGPSO method are defined according to the Table 1. The best solutions obtained by this method are the global maximum.

Pseudocode of the AGPSO algorithm

1: for $i \longleftarrow 1$ until Np do

2: Randomly initialize the position xi and the speed viof each particle;

3: Initialize the best position pi = xi;

4: Assess position xi;

5: Initialize pg, using the equation of the best global position;

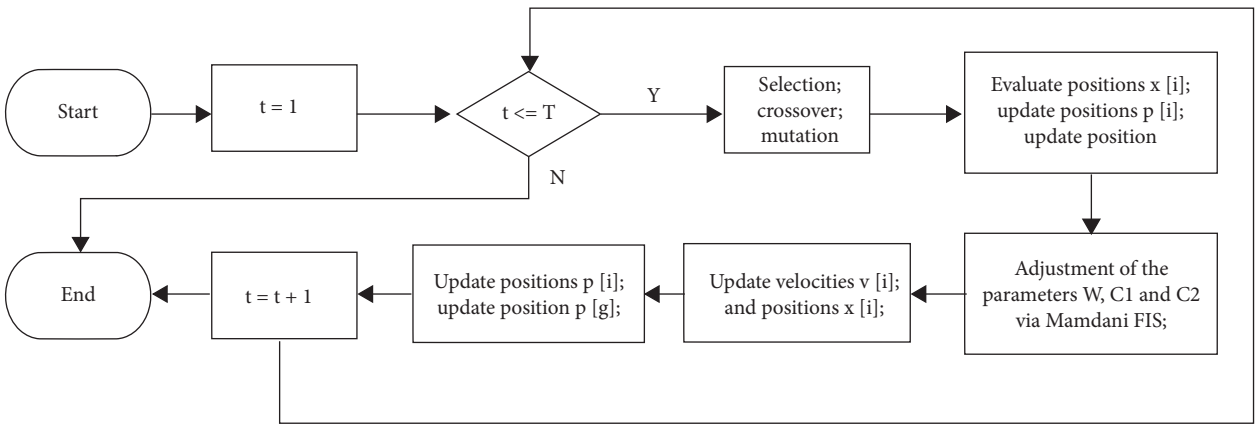

Figure 2: Adaptive GAPSO flowchart.

Table 1: General optimization parameters by the GAPSO method.

Populationsize	100 individuals
Numberof total iterations	100 iterations
Mutation rate	0.1 (10%)
Leniencyfee	0.5 (50%)
Inertia coefficient	1
Individual acceleration coefficient	1 (Initial)
Social acceleration coefficient	3 (Initial)

6: to end

7: for $t \longleftarrow 1$ until T do

8: for $i \longleftarrow 1$ until Np do

9: Select the particles that will be reproduced, with probability pc;

10: Apply the crossover;

11: Apply the mutation operator, with probability pm;

12: Insert new particles (children) into the population, replacing their parents;

13: Assess positions xi;

14: Update pi, using the equation of updating the position of each particle;

15: Update pg, using the equation of the best global position;

16: Update vi, using the equation of speed and best position, of each particle;

17: Update xi, using the speed update equation;

18: Evaluate positions xi;

19: Update pi, using the equation of updating the position of each particle;

20: Update pg, using the equation of the best global position;

21: end

22: end

4. Numerical Results

Based on the theory presented above, a MoM computational code was developed in the Matlab software to calculate the following results: input impedance, radiation diagram, radiation efficiency, gain, and directivity of the four nanoantennas and optimized via adaptive fuzzy GAPSO algorithm included in the MoM code. The objective function was defined as the maximum gain and radiation efficiency value of the YU antenna, given by

$$F(N_i) = \max(G(f, N_i).E(f, N_i)), \quad 100\,\text{THz} \le f \le 400\,\text{THz}, \tag{9}$$

where the N_i inputs of the objective function are the nanoantenna dimensions: length, radius, element distance, and dipole gap, which are contained in the search space, and are provided to the modeling algorithm.

4.1. Verification of the MoM Model. With the intention of testing and validating our MoM code developed, in this section, we present a comparison of the results obtained by FEM [18] and MoM codes. For this, we considered and simulated two antennas: a conventional YU array (Figure 1(a)) and an isolated dipole.

Figure 3 shows the input impedance calculated by MoM and FEM for both YU and isolated nanodipole for comparison, where this isolated nanodipole has the same dimensions of the nanodipole of the YU array. We observe a good agreement between these two methods and those reported in [11], which guarantees the good accuracy of our model. In both results, of isolated dipole and array, we note that the first two resonant frequencies are close each other; this shows that the directors and reflectors do not affect significantly the original resonant frequencies of the isolated dipole. The principal differences in these two cases is observed near the frequencies $F = 175$ and 260 THz (Figure 3(a)), which correspond physically to the dipolar resonances of the reflector and directors, respectively. These

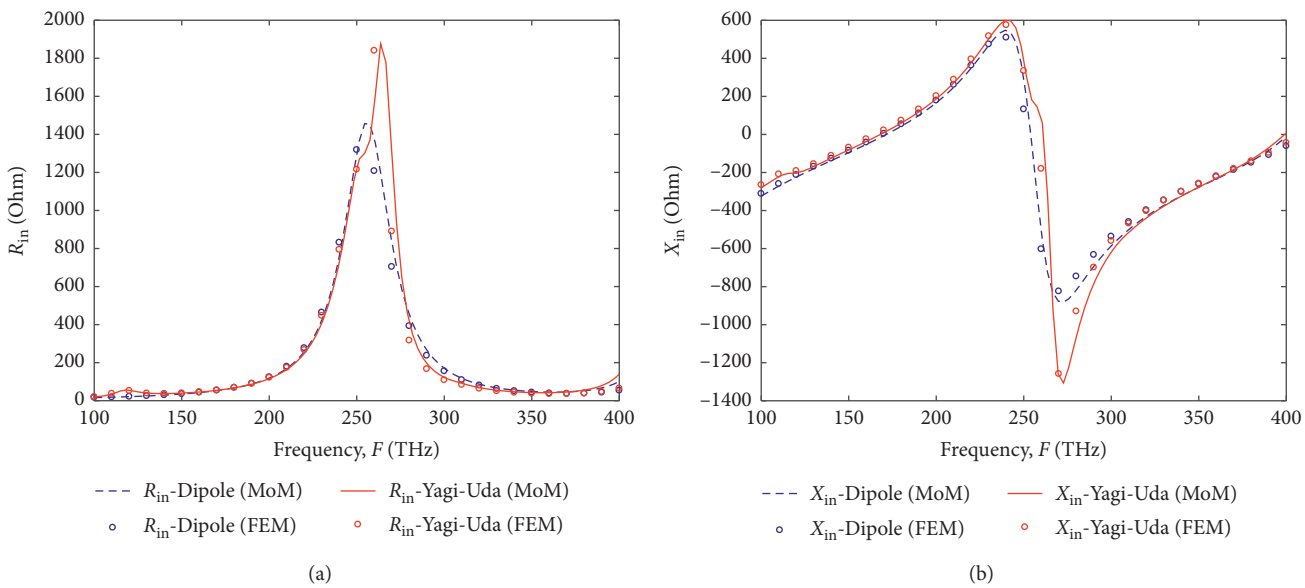

FIGURE 3: Input impedance of YU array and nanodipole: (a) R_{in} and (b) X_{in}. The dimensions of antennas are $h_r = 700$ nm, $h_t = 2$ (h) + (d) = 460 nm, $h_1 = h_2 = h_3 = 250$ nm, $d_h = d_1 = d_2 = d_3 = 100$ nm and $a_1 = a_2 = a_3 = a_h = a_r = 15$ nm.

resonances can be observed in the current distributions in these frequencies, which are not shown here.

4.2. Optimized Dimensions. To optimize the elements of YU nanoantennas, the search space of Table 2 was used. The search space is the range of the domain of the objective function in which the search for the minimum or maximum value of the function will be made. In this table are used typical values of dimensions considered in design of optical nanoantennas. The fuzzy adaptive AGPSO runs 100 iterations to find the best gain and efficiency of the nanoantennas.

Tables 3–6 show the optimized results obtained of the conventional YU (Figure 1(a)), YU with OTL (Figure 1(b)), YU with loop (Figure 1(c)), and YU with OTL and loop (Figure 1(d)), respectively. These tables present the optimized dimensions values of each element of the nanoantenna simulated by fuzzy adaptive AGPSO and the pertinence value equivalent to the maximum obtained gain of each nanoantenna.

In all the optimized antennas presented in these tables, the reflector and directors are smaller than the feeding element (dipole). We believe that this is due to the definition of the objective function being the gain instead of directivity. Smaller reflector size implies in smaller dissipated power in this element and consequently higher radiation efficiency. In this case, even that directivity been smaller, the higher efficiency compensates to obtain higher gain. In other words, smaller reflector produces higher efficiency, and the directors are responsible to increase the directivity.

4.3. Optimized Antenna Results. In this section, we present a comparison of the four nanoantennas optimized, in respect the following characteristics: input impedance, radiation efficiency, gain, and directivity, where their dimensions are presented in Tables 3–6.

Figure 4 presents the input impedances of the antennas, where Figure 4(a) shows the real component (R_{in}) and Figure 4(b) the imaginary component (X_{in}). In this figure, it is observed that the electromagnetic coupling between the YU nanoantenna with the new elements (OLT and Loop) modifies its input impedance. As the new elements are inserted in the YU, the larger is its input impedance in the frequency range of 200 THz to 260 THz. It is also observed that the nanoantenna YU and YU with OTL reached higher impedance value in the frequency range $F = 100$ to 150 THz (Figure 4(a)). The nanoantennas YU with loop and YU with loop and OTL reached higher values of R_{in} in the frequency range $F = 180$ to 280 THz (Figure 4(a)).

Figure 5 shows the radiation efficiency results e_r, in function of frequency. The adaptive fuzzy GAPSO optimization show to be effective when applied in nanoantennas design. In this work, good results are obtained: maximum efficiency of $e_r = 0.80$ for the YU with OTL and loop, $e_r = 0.73$ for the YU with loop, $e_r = 0.57$ for the YU with OTL, and $e_r = 0.53$ for the conventional YU. It is observed that in the insertion of new elements (OTL and loop) in the conventional YU, and after the optimization process, the resulted are improved considerably as can be seen in Figure 5.

Figure 6 shows the results of directivity (Figure 6(a)) and gain (Figure 6(b)) of the four optimized YU in the $+y$ direction. We observe that, in Figure 6(a), the maximum value of the directivity occurred in the case of YU with OTL and loop, where a peak of $D_0 = 46.5$ was obtained close to 259 THz. In the other hand, for the case of YU with loop, we have a peak of $D_o = 31.7$ near 274 THz, but at this frequency, the radiation efficiency is $e_r = 0.1$, which consequently reduces the gain because $G_0 = e_r D_0$. Table 7 shows the maximum directivity of the four nanoantennas and the frequency

Table 2: Search space for each dimension of the elements of the conventional YU nanoantenna.

Dipole			Transmission line (when present)			
Arm length (nm)		Radius (nm)	Length (nm)	Radius (nm)	Gap (nm)	
90–330		10–30	500–1000	10–30	10–30	
Reflector and directors			Rectangular loop (when present)			
Length (nm)	distance (nm)	Radius (nm)	Length (nm)	Distance (nm)	Radius (nm)	Height (nm)
90–330	90–330	10–30	400–1000	50–100	10–30	0–50

Table 3: Optimal dimensions found by fuzzy adaptive AGPSO method for conventional YU nanoantenna.

Dipole			1° director		
Arm length (nm)	Radius (nm)		Length (nm)	Distance (nm)	Radius (nm)
260	27		285	291	30
Reflector			2° director		
Length (nm)	Distance (nm)	Radius (nm)	Length (nm)	Distance (nm)	Radius (nm)
254	267	29	281	283	30
3° director			Pertinence (gain)		
Length (nm)	Distance (nm)	Radius (nm)			
280	290	28	5		

Table 4: Optimal dimensions found by the fuzzy adaptive AGPSO method for YU nanoantenna connected to a transmission line.

Dipole			1° director		
Arm length (nm)	Radius (nm)		Length (nm)	Distance (nm)	Radius (nm)
272	16	300	90	25	
Reflector			2° director		
Length (nm)	Distance (nm)	Radius (nm)	Length (nm)	Distance (nm)	Radius (nm)
300	300	23	300	300	25
3° director			Transmission line		
Length (nm)	Distance (nm)	Radius (nm)	Length (nm)	Radius (nm)	Gap (nm)
300	300	25	500	30	30
Pertinence (gain)					
7.6					

Table 5: Optimal dimensions found by the fuzzy adaptive AGPSO method for YU nanoantenna combined to a rectangular loop.

Dipole			1° director		
Arm length (nm)	Radius (nm)		Length (nm)	Distance (nm)	Radius (nm)
280	20		300	300	25
Reflector			2° director		
Length (nm)	Distance (nm)	Radius (nm)	Length (nm)	Distance (nm)	Radius (nm)
300	300	20	300	300	25
3° director			Rectangular loop		
Length (nm)	Distance (nm)	Radius (nm)	Length (nm)	Distance (nm)	Radius (nm)	Height (nm)
300	300	25	610	60	25	30
Pertinence (gain)						
7.8						

Table 6: Optimal dimensions found by the fuzzy adaptive AGPSO method for YU nanoantenna connected to a transmission line and combined with a rectangular loop.

Dipole			1° director		
Arm length (nm)	Radius (nm)		Length (nm)	Distance (nm)	Radius (nm)
280	20		300	95	25
Reflector			2° director		
Length (nm)	Distance (nm)	Radius (nm)	Length (nm)	Distance (nm)	Radius (nm)
300	300	20	300	300	25
3° director			Rectangular loop		
Length (nm)	Distance (nm)	Radius (nm)	Length (nm)	Distance (nm)	Radius (nm)	Height (nm)
300	300	25	720	60	25	30
Transmission line			Pertinence (Gain)			
Length (nm)	Radius (nm)	Gap (nm)				
500	26	28	9.6			

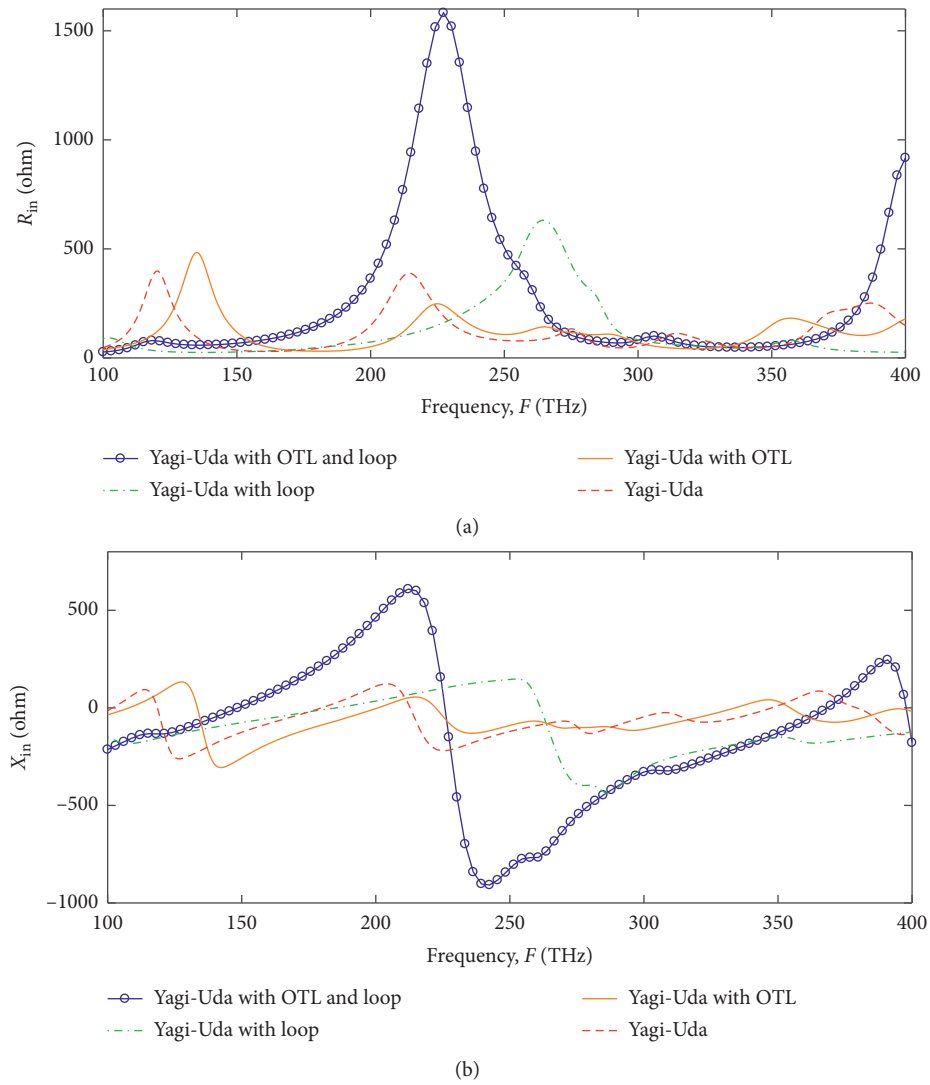

Figure 4: Variation of input impedance in frequency of the four YU nanoantennas: (a) R_{in} and (b) X_{in}.

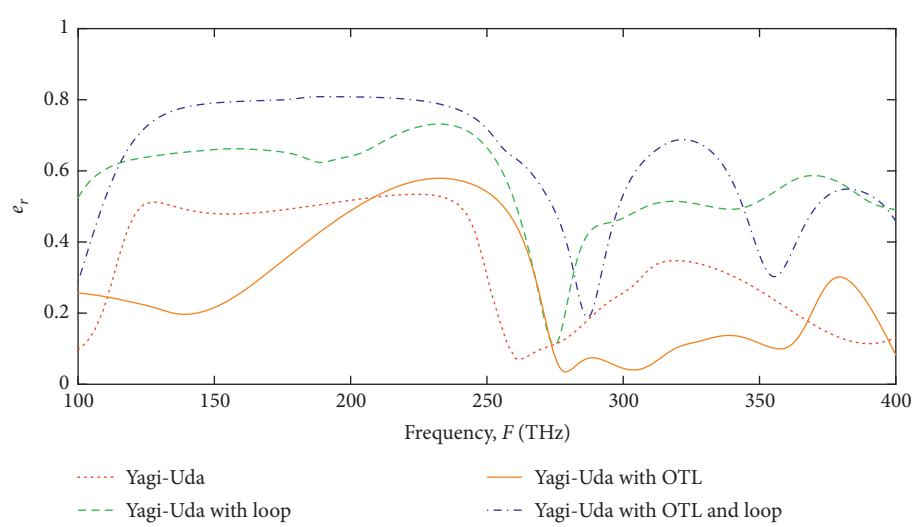

Figure 5: Radiation efficiency e_r of the four optimized YU nanoantennas.

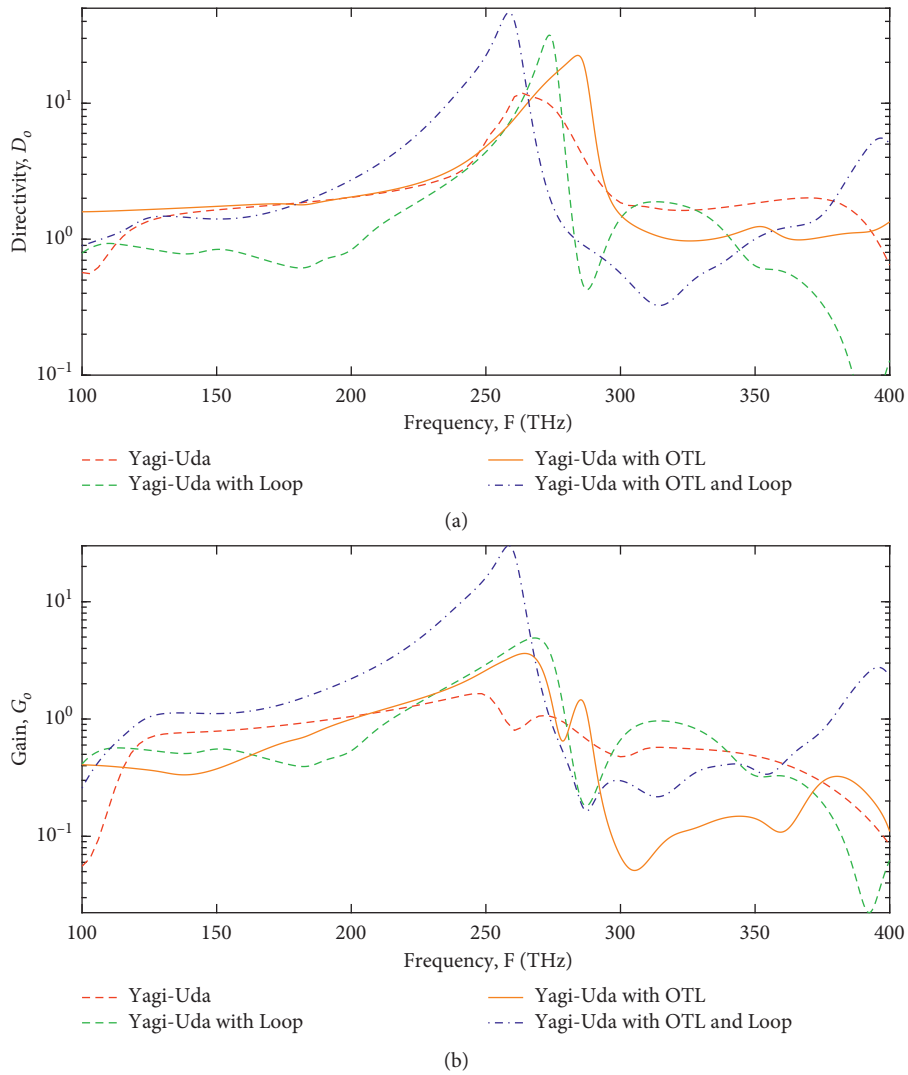

Figure 6: Directivity $(D)_0$ (a) and gain $(G)_0$ (b) of the four optimized YU nanoantennas.

Table 7: Resonance frequency and peak values of directivity of the four nanoantennas.

Nanoantenna	Frequency (THz)	D_0
Yagi-Uda	264	11.8
Yagi-Uda with OTL	284	22.5
Yagi-Uda with Loop	274	31.7
Yagi-Uda with OTL and Loop	259	46.5

Table 8: Resonance frequency and peak values of gain of the four nanoantennas.

Nanoantenna	Frequency (THz)	G_0
Yagi-Uda	247	1.65
Yagi-Uda with OTL	264	3.62
Yagi-Uda with Loop	268	4.91
Yagi-Uda with OTL and Loop	259	30

where it occurs. We observe from this table that the nanoantennas OTL and loop presented higher directivity than the other cases with OTL.

The maximum gain is also improved with the inclusions of these elements, as can be viewed in Table 8, where the gain of the conventional YU is increased from $G_0 = 1.65$ to 3.62 with the addition of the OTL and increases to 1.65 and 4.91 with the addition of the loop, and 1.65 to 30 for the case with loop and OTL.

5. Conclusions

In this paper, we presented the optimization of some radiation and absorption characteristics of four types of modified Yagi-Uda (YU) nanoantennas. The optimization technique used is the hybrid adaptive fuzzy GAPSO method. The results showed, in overall, that the insertion of new elements, such as loop elements and optical transmission line, in the geometry of the classic YU nanoantenna

produced improved values of efficiency, directivity, and gain when compared to the conventional one. It was also observed that the variation in spacing and dimensions of the elements considerably modifies the magnitude of directivity and gain. Another important conclusion obtained is that, for any YU antenna considered, the maximum gain does not necessarily occurs in the same frequency of maximum directivity. This means that the operation point depends in which characteristic directivity or gain that is more important in a given application. And finally, we observed that the adaptive fuzzy GAPSO is capable of optimizing any objective function with minimal restrictions. This makes this method an extremely versatile tool for modeling/optimization complex problems of nanoantennas.

Regarding the advantages of the nanoantennas proposed in this work, we observed that in general the performance of these are better than the conventional YU antenna, without significantly increasing their total size. These results may be useful for the design of efficient and compact YU nanoantennas for nanoplasmonic applications. The only disadvantage was the small increase in the overall input impedance of the proposed antennas compared to the conventional YU nanoantenna. In the future works, we intend to apply this optimization method in YU nanoantennas fed by Gaussian beam and optimize the impedance matching of these nanoantennas with optical transmission lines.

Data Availability

The data used to support this study can be available upon request to the corresponding author.

Conflicts of Interest

The authors declare that they have no conflicts of interest.

References

[1] P. Bharadwaj, B. Deutsch, and L. Novotny, "Optical antennas," *Advances in Optics and Photonics*, vol. 1, no. 3, pp. 438–483, 2009.

[2] L. Novotny and N. Van Hulst, "Antennas for light," *Nature Photonics*, vol. 5, no. 2, pp. 83–90, 2011.

[3] A. Alu and N. Engheta, "Theory, modeling and features of optical nanoantennas," *Institute of Electrical and Electronics Engineers Transactions on Antennas and Propagation*, vol. 61, no. 4, pp. 1508–1517, 2013.

[4] I. S. Maksymov, I. Staude, A. E. Miroshnichenko, and Y. S. Kivshar, "Optical Yagi-Uda nanoantennas," *Journal of Nanophotonics*, vol. 14, 2012.

[5] Q. Gao, S. Liverman, and A. X. Wang, "Design and characterization of high efficiency nanoantenna couplers with plasmonic integrated circuit," *Journal of Lightwave Technology*, vol. 35, no. 15, pp. 3182–3188, 2017.

[6] F. Obelleiro, J. M. Taboada, D. M. Solís, and L. Bote, "Directive antenna nanocoupler to plasmonic gap waveguides," *Optics Letters*, vol. 38, no. 10, pp. 1630–1632, 2013.

[7] E. G. Mironov, A. Khaleque, L. Liu, I. S. Maksymov, and H. T. Hattori, "Enhancing weak optical signals using a plasmonic yagi-uda nanoantenna array," *Institute of Electrical and Electronics Engineers Photonics Technology Letters*, vol. 26, no. 22, pp. 2236–2239, 2014.

[8] T. Kosako, Y. Kadoya, and H. F. Hofmann, "Directional control of light by a nano-optical yagi-uda antenna," *Nature Photonics*, vol. 4, no. 5, pp. 312–315, 2010.

[9] I. S. Maksymov, A. E. Miroshnichenko, and Y. S. Kivshar, "Actively tunable bistable optical Yagi-Uda nanoantenna," *Optics Express*, vol. 20, no. 8, pp. 8929–8938, 2012.

[10] K. Q. da Costa, G. T. C. de Sousa, P. R. Amaral, J. L. Souza, and P. N. dos Santos, "Wireless optical nanolinks with yagi-uda and dipoles plasmonic nanoantennas," *Nanoplamonics: Chapter 1*, Intech Open, London, UK, 2019.

[11] K. Q. Da Costa and V. Dmitriev, "Simple and efficient computational method to analyze cylindrical PlasmonicNanoantennas," *International Journal of Antennas e Propagation*, vol. 2014, Article ID 675036, 8 pages, 2014.

[12] U. Singh and R. Salgotra, "Pattern synthesis of linear antenna arrays using enhanced flower pollination algorithm," *International Journal of Antennas and Propagation*, vol. 2017, Article ID 7158752, 11 pages, 2017.

[13] R. Salgotra, U. Singh, S. Saha, and A. K. Nagar, "Improved flower pollination algorithm for linear antenna design problems," in *Soft Computing for Problem Solving. Advances in Intelligent Systems and Computing*, K. Das, J. Bansal, K. Deep, A. Nagar, P. Pathipooranam, and R. Naidu, Eds., vol. 1048, Springer, 2020.

[14] R. Salgotra, U. Singh, and S. Saha, "On some improved versions of whale optimization algorithm," *Arabian Journal for Science and Engineering*, vol. 44, no. 11, pp. 9653–9691, 2019.

[15] R. Salgotra and U. Singh, "The naked mole-rat algorithm," *Neural Computing and Applications*, vol. 31, no. 12, pp. 8837–8857, 2019.

[16] U. Singh, R. Salgotra, and M. Rattan, "A novel binary spider monkey optimization algorithm for thinning of concentric circular antenna arrays," *The Institution of Electronics and Telecommunication Engineers Journal of Research*, vol. 62, no. 6, pp. 736–744, 2016.

[17] Z. Michalewicz and M. Schoenauer, "Evolutionary algorithms for constrained parameter optimization problems," *Evolutionary Computation*, vol. 4, no. 1, pp. 1–32, 1996.

[18] COMSOL Inc., *COMSOL Multiphysic 4.4a*, COMSOL Inc., Bengaluru, India, 2013, http://www.comsol.com/.

[19] L. Novotny and B. Hecht, *Principles of Nano-Optics*, University of Cambridge, Cambridge, UK, 2 edition, 2012.

[20] K. Q. da Costa and E V. Dmitriev, "Software based on mom model to analyze electromagnetic transients in grounding systems," in *Proceedings of the International Conference on Grounding e Earthing& 2nd International Conference on Lightning Physics e Effects*, Manaus, Brazil, November 2006.

[21] J. H. Holle, "Genetic algorithms e adaptation," in *Adaptive Control of Ill-Defined Systems. NATO Conference Series (II Systems Science)*, O. G. Selfridge, E. L. Rissle, and A. ArbibM, Eds., Vol. 6, Springer, Boston, MA, USA, 1984.

[22] B. L. Miller and D. E. E Goldberg, "Genetic algorithms, tournament selection, and the effects of noise," *Complex System*, vol. 9, pp. 193–212, 1995.

[23] T. Higuchi, S. E Tsutsui, and M. Yamamura, "Theoretical analysis of simplex crossover for real-coded genetic algorithms," in *Parallel Problem Solving From Nature. PPSN VI. PPSN 2000. Lecture Notes in Computer Science*, M. Schoenauer et al., Ed., Vol. 1917, Springer, Berlin, Heidelberg, 2000.

[24] T. Yalcinoz and H. A. M. Uzam, "Economic dispatch solution using a genetic algorithm based on arithmetic crossover," in *Proceedings of the 2001 IEEE Porto Power Tech Proceedings (Cat. No. 01EX502)*, vol. 2, p. 4, Porto, Portugal, September 2001.

[25] W. M. Spearse, K. D. D. Jong, *On the Virtues of Parametrized Uniform Crossover*, Morgan Kaufman Publishing, Burlington, MA, USA, 1995.

[26] J. Hesser and R. Manner, "Towards an optimal mutation probability for genetic algorithms," in *Proceedings of the 1st Workshop on Parallel Problem Solving from Nature PPSN I*, pp. 23–32, Dortmund, Germany, October 1990.

[27] L. A. Zader, "Fuzzy logic, neural networks, and soft computing," *Communications of the ACM Association for Computing Machinery, Inc.*vol. 37, no. 3, pp. 77–85, 1994.

[28] E. H. Mamdani and S. Assilian, "An experiment in linguistic synthesis with a fuzzy logic controller," *International Journal of Man-Machine Studies*, Elsevier, vol. 7, no. 1, pp. 1–13, 1975.

[29] T. Tagaki and M. Sugeno, "Fuzzy identification of systems e its applications to modeling e control," *Institute of Electrical and Electronics Engineers Transactions on Systems, Man, E Cybernetics. Institute of Electrical and Electronics Engineers*, vol. 1, pp. 116–132, 1985.

[30] R. Eberhart and J. Kennedy, "A new optimizer using particle swarm theory," in *Proceedings of the IEEE Micro Machine e Human Science, 1995, MHS'95, Proceedings of the Sixth International Symposiu on*, pp. 39–43, Nagoya, Japan, October 1995.

[31] A. P. Engelbrecht, *Computational Intelligence: An Introduction*, John Wiley & Sons, Hoboken, NJ, USA, 2007.